AD-A039 857 COLORADO STATE UNIV FORT COLLINS DEPT OF CHEMISTRY F/G 20/2
VIBRATIONAL SPECTRA OF TRANSITION METAL HEXAFLUORIDE CRYSTALS. --ETC(U)
APR 77 E R BERNSTEIN, G R MEREDITH N00014-75-C-1179

UNCLASSIFIED TR-13 NL

1 OF 1
AD A039 857

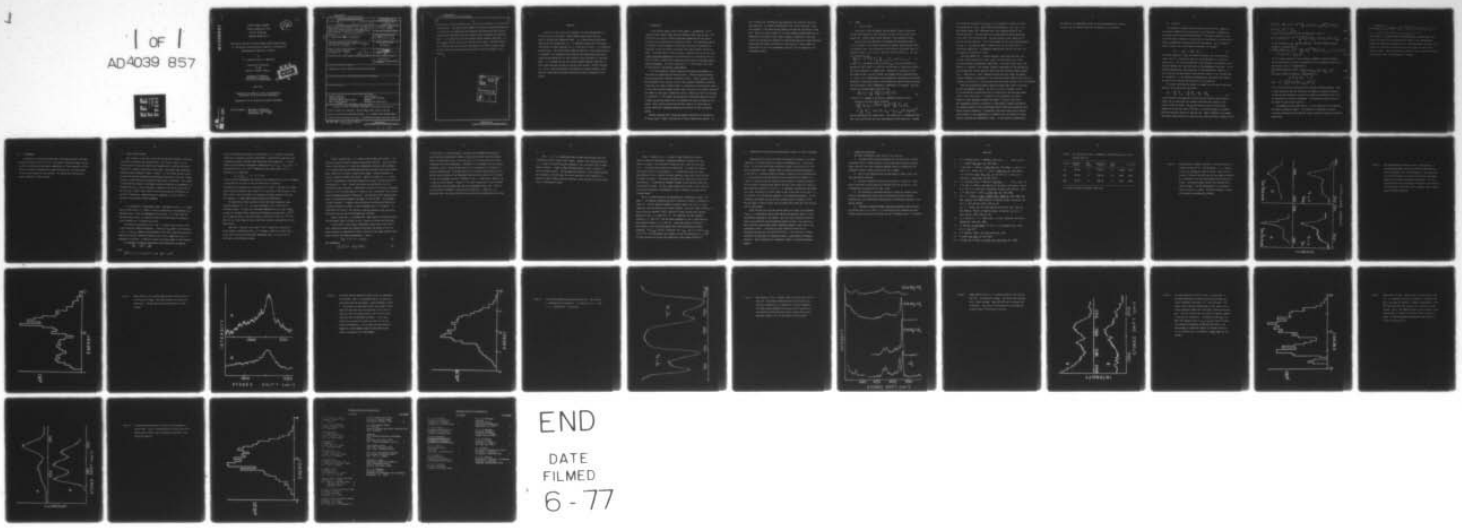

END

DATE
FILMED
6-77

FG.

12

OFFICE OF NAVAL RESEARCH

Contract N00014-75-C-1179

Task No. NR 056-607

TECHNICAL REPORT NO. 13

"Vibrational Spectra of Transition Metal Hexafluoride Crystals. II. Two-Particle and Mixed Crystal Spectra as Techniques For Determination of Densities of States"

by

E. R. Bernstein and G. R. Meredith*

Prepared for Publication
in the
Journal of Chemical Physics

Department of Chemistry
Colorado State University
Fort Collins, Colorado 80523

April 1977

*Current address: Department of Chemistry
University of Pennsylvania
Philadelphia, PA 19174

UNCLASSIFIED

SECURITY CLASSIFICATION OF THIS PAGE (When Data Entered)

REPORT DOCUMENTATION PAGE

READ INSTRUCTIONS BEFORE COMPLETING FORM

1. REPORT NUMBER: 13
2. GOVT ACCESSION NO.:
3. RECIPIENT'S CATALOG NUMBER: TR-13

4. TITLE (and Subtitle): Vibrational Spectra of Transition Metal Hexafluoride Crystals. II. Two-Particle and Mixed Crystal Spectra as Techniques for Determination of Densities of States.

5. TYPE OF REPORT & PERIOD COVERED: Technical Report

6. PERFORMING ORG. REPORT NUMBER:

7. AUTHOR(s): E. R. Bernstein and G. R. Meredith

8. CONTRACT OR GRANT NUMBER(s): N00014-75-C-1179

9. PERFORMING ORGANIZATION NAME AND ADDRESS: Colorado State University, Dept. of Chemistry, Fort Collins, CO 80523

10. PROGRAM ELEMENT, PROJECT, TASK AREA & WORK UNIT NUMBERS: NR 056-607

11. CONTROLLING OFFICE NAME AND ADDRESS: Office of Naval Research, Arlington, VA 22217

12. REPORT DATE: April 1977

13. NUMBER OF PAGES: 45

14. MONITORING AGENCY NAME & ADDRESS (if different from Controlling Office):

15. SECURITY CLASS. (of this report): Unclassified

15a. DECLASSIFICATION/DOWNGRADING SCHEDULE:

16. DISTRIBUTION STATEMENT (of this Report)

Approved for Public Release; Distribution Unlimited.

17. DISTRIBUTION STATEMENT (of the abstract entered in Block 20, if different from Report)

18. SUPPLEMENTARY NOTES

19. KEY WORDS (Continue on reverse side if necessary and identify by block number)

Raman scattering
molecular crystals
transition metal hexafluorides
pure crystal spectra
mixed crystals
exciton band structure
phonons
two-particle transitions

20. ABSTRACT (Continue on reverse side if necessary and identify by block number)

In part II of this series two techniques for obtaining densities of exciton states are discussed: heavily doped mixed crystals and two-particle overtone and combination bands. It is demonstrated through Raman spectra and calculations that (ν_i + ν_j) combination bands yield very nearly

DD FORM 1 JAN 73 1473 EDITION OF 1 NOV 65 IS OBSOLETE S/N 0102-014-6601

UNCLASSIFIED

SECURITY CLASSIFICATION OF THIS PAGE (When Data Entered)

404 992

20.

true density of states functions for ν_i in the case for which ν_1 is essentially dispersionless. The mixed crystal method for density of states determinations is compared to the combination band technique and approximate mixed crystal concentrations appropriate for such studies can be calibrated for individual bands. It is pointed out that the overtone method, whenever applicable, is both simpler and more accurate for exciton state studies. Detailed analyses of ν_1 and $2\nu_1$ show that the major contribution to overtone intensity comes from the second order polarizability derivative and not anharmonic contributions.

Abstract

In part II of this series two techniques for obtaining densities of exciton states are discussed: heavily doped mixed crystals and two-particle overtone and combination bands. It is demonstrated through Raman spectra and calculations that $(\nu_i + \nu_1)$ combination bands yield very nearly true density of states functions for ν_i in the case for which ν_1 is essentially dispersionless. The mixed crystal method for density of states determinations is compared to the combination band technique and approximate mixed crystal concentrations appropriate for such studies can be calibrated for individual bands. It is pointed out that the overtone method, whenever applicable, is both simpler and more accurate for exciton state studies. Detailed analyses of ν_1 and $2\nu_1$ show that the major contribution to overtone intensity comes from the second order polarizability derivative and not anharmonic contributions.

I. INTRODUCTION

In the previous paper in this series (paper I, preceeding)[1], we discussed the neat crystal single particle spectra of MoF_6, WF_6, and UF_6. The similarities and trends in these systems were emphasized and the spectra were seen to be characteristic of molecular solids. The vibrational spectra of molecular crystals generally display sharp structure corresponding to elementary crystal excitations associated with single molecule vibrational modes. The predominance of this structure is generally due to the fact that crystal transition operators are associated with first order derivatives of electric dipole or polarizability operators with respect to molecular vibrational coordinates. The latter cause only $\Delta v = \pm 1$ vibrational transitions of the molecule in the harmonic approximation.

In isolated molecules, weaker features are observed corresponding to transitions to combination and overtone levels. These multiple excitations may be qualitatively different in molecular solids. Loosely speaking, they may correspond to the creation of two or more separate elementary excitations rather than one single excitation which is associated with the molecular level. In ionic and covalently bonded crystals these transitions are commonly observed;[2] the number of such cases in molecular crystals, though very small not long ago, is increasing.[3] In this paper the two-particle (two-phonon) Raman excitations in MoF_6, WF_6 and UF_6 crystals will be presented and intensity mechanisms discussed. Under certain restrictions the basic density of states shape of various vibrational fundamental bands may be observed in these two-phonon spectra.

Another technique which allows experimental observation of the density of states shape is based on the spectra of heavily doped mixed crystals. In

such a system (say, 25% MoF_6/75% UF_6) wavevector ($\underline{k}$) selection rules have been destroyed. An inherent disadvantage of this latter technique is that the perturber of the translational symmetry also perturbs the details of the band. Spectra of mixed crystals of the three systems mentioned above will be presented and discussed in this light, allowing a comparison of the mixed crystal and two-particle techniques for determining density of states functions. Electrostatic multipolar calculations of the density of states (paper III, following)[4] for two of the fundamental bands will also be compared to the experimental shapes.

II. THEORY

A. Crystal States

Discussions of the one-phonon[5] and two-phonon[6] states of molecular crystals have appeared in the literature, so only a brief review is presented here. Greater detail may be obtained in the references cited.

Assuming that the separation of one-phonon and two-phonon states is a valid concept for the crystal system being studied, the one-phonon states are generated from a set of molecular site functions (χ^f_{nq}) which covers all molecular levels f, unit cells n, and sites in the unit cells q. The one-site exciton functions

$$\phi^f_q(\underline{k}) = N^{-1/2} \sum_n \chi^f_{nq} \prod_{n'q' \neq nq} \chi^0_{n'q'} \exp(i\underline{k}\cdot\underline{r}_{nq}), \qquad (1)$$

in which N is the number of unit cells and $\underline{r}_{nq}$ is a position vector, are defined for the Z sites in a unit cell and are used as a basis set in which the crystal potential is diagonalized. Wavevector is conserved so that the dynamical matrix can be factored into diagonal blocks characterized by $\underline{k}$. Usually, for isolated modes, the intramolecular vibrations may be treated separately so that each $\underline{k}$ block is partitioned into smaller blocks involving only one molecular level (fundamental, combination, or overtone). One then obtains the isolated band exciton functions

$$\phi^f_\alpha(\underline{k}) = \sum_{qf'} B^{ff'}_{\alpha q}(\underline{k})\, \phi^{f'}_q(\underline{k}), \qquad (2)$$

in which f' is a member of the possibly degenerate molecular level.

Similarly, two-site exciton functions

$$\phi^{fg}_{qp}(\underline{k}_f, \underline{k}_g) = [N(N-\delta_{qp})]^{-1/2} \sum_{nm} \chi^f_{nq}\chi^g_{mp} \times \prod'_{n'q'} \chi^0_{n'q'} \exp(i\underline{k}_f\cdot\underline{r}_{nq} + i\underline{k}_g\cdot\underline{r}_{mp})(1-\delta_{qp}\delta_{nm}) \qquad (3)$$

may be constructed as a crystal basis. The restriction is incorporated that the f and g excitations not occur simultaneously on the same site. Instead

of the separate wavevectors $\underline{k}_f$ and $\underline{k}_g$, it is convenient to define the difference wavevector $\underline{K} = \frac{1}{2}(\underline{k}_f - \underline{k}_g)$ and the total wavevector $\underline{k} = \underline{k}_f + \underline{k}_g$. $\underline{k}$ is a good quantum number and so characterizes a block diagonalization of the Hamiltonian matrix. For each value of $\underline{k}$, $\underline{K}$ may take on N values equivalent to the total first Brillouin zone. For each value of $\underline{k}$ and $\underline{K}$ there are Z^2 two-site exciton functions. Even if one assumes $\underline{K}$ to be a good quantum number[6] and uses an isolated band model, diagonalization of the Hamiltonian is a significant undertaking. A reasonable approximation might be the direct sum of energies of one-particle states.

The large number of $\underline{k} = 0$ states and their large band width make transitions to these two-particle states readily distinguishable from single particle overtone and combination transitions. The latter display only a few narrow $\underline{k} = 0$ features. The transfer integrals responsible for the two-particle exciton bands must involve operators which move two vibrational quanta between sites. Additionally, a small anharmonicity may allow the larger one quantum transfer integrals to contribute to the two-particle band; however,these terms are reduced by the square of a mixing coefficient (one factor for each site in the integral

When the one-phonon/two-phonon separation breaks down, there are two ways to solve the dynamical problem. The first is to set up general $\underline{k}$ blocks of the Hamiltonian including both sets of crystal basis functions and diagonalize in this larger basis. A variation of this procedure, the second method, has been suggested by Rashba and Sheka,[7] in which interaction of two independent elementary excitations is described by a general Hamiltonian. The coupling problem is then solved under certain simplifying assumptions with Greens function techniques.[7] An important point which stems from an analysis such as theirs is that anharmonicity is essential for the creation of single particle (overtone and combination) states. In the absence of anharmonicity

the particles are independent except for small perturbations of transfer integrals and site energies when the excitations are in proximity.

B. Intensity

The appearance of Raman scattering intensity at molecular combination and overtone frequencies has two sources in free molecules: anharmonicity and higher order polarizability derivatives.[8] The general treatment of the scattering process reduces to the evaluation of the electronic polarizability tensor $\underline{\underline{\alpha}}_m$ between two scattering states of the molecule. $\underline{\underline{\alpha}}_m$ is assumed to depend parametrically on the normal coordinates, for instance

$$\underline{\underline{\alpha}}_m = \underline{\underline{\alpha}}_m^c + \underline{\underline{\alpha}}'_{mi} Q_{mi} + \cdots \quad . \tag{4}$$

The implied summation is over all normal coordinates, but within one electronic level it is effectively over only the gerade modes if an inversion center exists. The nuclear coordinates in this expansion are operators to be evaluated between the vibrational parts of Born-Oppenheimer functions. In the harmonic approximation, the second term in the expansion will cause $\Delta v = \pm 1$ transitions and the much smaller third term will cause $\Delta v = 0, \pm 2$ transitions (or scattering). In the presence of anharmonicity, the latter type scattering may also be caused by the second term of the expansion.

The crystal polarizability tensor is assumed to be the sum of individual molecular (site) polarizability tensors

$$\underline{\underline{\alpha}}_c = \sum_{nq} \underline{\underline{\alpha}}_{nq} = \sum_{nq} \underline{\underline{D}}_{nq} \cdot \underline{\underline{\alpha}}_m \cdot \underline{\underline{D}}^+_{nq} \tag{5}$$

in which the last term expresses the fact that the molecular polarizability tensors are all equivalent but oriented differently with respect to the crystal fixed axis system. The $\underline{\underline{D}}_{nq}$ are unitary rotation matrices which depend only on the site label q, but the n is carried through as a reminder that each term only operates in one unit cell. Matrix elements of $\underline{\underline{\alpha}}_c$ between the crystal ground state and a single particle state described by equation 2 are

$$\langle \phi^o | \underline{\underline{\alpha}}_c | \phi^f_\alpha(\underline{k}) \rangle = N^{-1/2} \sum_{nqf'} \exp(i\underline{k}\cdot\underline{r}_{nq}) B^{ff'}_{\alpha q}(\underline{k}) \underline{\underline{D}}_{nq} \cdot \langle \chi^o | \underline{\underline{\alpha}}_m | \chi^{f'} \rangle \cdot \underline{\underline{D}}^+_{nq} \tag{6a}$$

in which the equivalence of sites has been used. For $\underline{k} = 0$

$$\langle \phi^o | \underline{\underline{\alpha}}_c | \phi^f_\alpha(\underline{k}) \rangle = N^{+1/2} \sum_{qf'} B^{ff'}_{\alpha q}(0) \underline{\underline{D}}_{oq} \cdot \langle \chi^o | \underline{\underline{\alpha}}_m | \chi^{f'} \rangle \cdot \underline{\underline{D}}^+_{oq} . \tag{6b}$$

In (6b) the equality $\underline{\underline{D}}_{nq} = \underline{\underline{D}}_{0q}$ has been used. The total Raman scattering intensity is proportional to

$$|\langle \phi^o | \underline{\underline{\alpha}}_c | \phi^f_\alpha(\underline{k}) \rangle \cdot \underline{E}|^2 = N \sum_{qf'f''} B^{ff''*}_{\alpha q} B^{ff'}_{\alpha q} |\underline{E}\cdot\underline{\underline{D}}_{oq} \cdot \langle \chi^o | \underline{\underline{\alpha}}_m | \chi^{f''} \rangle^+ \cdot \langle \chi^o | \underline{\underline{\alpha}}_m | \chi^{f'} \rangle \cdot \underline{\underline{D}}^+_{oq} \cdot \underline{E}| . \tag{7a}$$

The total Raman intensity in the sZ Davydov components (ignoring frequency factors and summing f over the s degenerate or nearly degenerate functions of the molecular basis) is proportional to

$$\sum_{f\alpha} |\langle \phi^o | \underline{\underline{\alpha}}_c | \phi^f_\alpha(0) \rangle \cdot \underline{E}|^2 = N \sum_{f'q} |\langle \chi^o | \underline{\underline{\alpha}}_m | \chi^{f'} \rangle \cdot \underline{\underline{D}}^+_{oq} \cdot \underline{E}|^2 . \tag{7b}$$

The scalar scattering intensity is proportional to

$$N_s Z \alpha_s^2 |\underline{E}|^2 = G_o^2 \tag{7c}$$

with $\alpha_s^2 = \sum_{f'} \left| \sum_i \langle \chi^o | (\alpha_m)_{ii} | \chi^{f'} \rangle \right|^2 .$

This is just the scalar scattering of NsZ randomly oriented molecules. Such a simple expression does not follow for the symmetric scattering intensity. In that case the expression is the sum of scattering intensities from Z sets of N molecules at definite orientations. The resultant scattering must be evaluated for each crystal structure.

The comment should be made that Eq. 7a is an expression of the (possibly distorted) oriented gas model.[9] The scattering is dependent on crystal structure and molecular polarizability tensors (and hence molecular transition mechanisms).

By noting that

$$\langle \Phi^{o} | \underline{\underline{\alpha}}_{c} | \Phi^{fq}_{qp}(\underline{k}_{f}, \underline{k}_{q}) \rangle = \left[N(N - \delta_{qp}) \right]^{-1/2} \sum_{n,q'} \sum_{nm} \left\{ \langle \chi^{o}_{nq} \chi^{o}_{mp} | \underline{\underline{\alpha}}_{n,q'} | \chi^{f}_{nq} \chi^{3}_{mp} \rangle \right.$$

$$\left. \chi (1 - \delta_{qp} \delta_{nm}) \right\} \exp\left(i \underline{k}_{f} \cdot \underline{r}_{nq} + i \underline{k}_{q} \underline{r}_{mp} \right) = 0$$

because the { } bracketed term is identically zero, one sees there is no scattering intensity to pure two-particle states in this approximation. Rather than challenge the adequacy of eq. 5 one would expect intensity to be brought into two-particle transitions by a mixing with the pure single particle states. This mixing preserves the total scalar scattering intensity over the set of one- and two-phonon $\underline{k} = 0$ states.

III. EXPERIMENTAL

The details of crystal preparation and of the Raman apparatus have been discussed in paper I and in ref. 10. The crystals studied were MoF_6, WF_6 and UF_6 neat crystals and various binary combinations of these compounds as mixed crystals in nominal concentrations ranging from less than five mole percent to greater than ninety-five mole percent. All spectra were obtained with samples immersed in liquid nitrogen.

IV. RESULTS AND DISCUSSION

Many features in the neat crystal spectra have been assigned to molecular vibrational combination and overtone bands. The overall breadth, lack of structure, and in some cases, significant frequency shifts indicate that these features are generally two-particle transitions. The bending mode combination region has been presented in paper I, Figure 7. In this paper we wish to deal specifically with the combinations and overtones involving at least one stretching mode, largely because the spectra are more easily interpreted. This section is organized with respect to individual molecular vibrations as fundamentals, as combinations with ν_1, and as overtones. Inherent in this entire discussion is the fact that, despite small crystal structure and molecular differences, the excitonic interactions, though different in magnitude, are quite similar in nature for the crystals of these compounds.

A. ν_1

ν_1 is essentially a dispersionless band. The widths of the $\nu_1 = 2\ \nu_1$ bands and the shifts from $2 \times \nu_1$ (Table 1) serve as indications of the bandwidths and anharmonicities. Since the anharmonicities are small, it is likely that the increased width of the $2\ \nu_1$ features is due to the convolution of the band on itself generating $\underline{k} = 0$ two-particle states.

The relative intensities of the ν_1 and $2\ \nu_1$ bands can be used as a test of the scattering intensity mechanisms. In the O_h or D_{4h} models of the molecule, ν_1 and $2\ \nu_1$ have a_{1g} symmetry and consequently only scalar scattering mechanisms. Therefore the scalar scattering intensity (Sect. IIB.), summed over the $\underline{k} = 0$ components of the band, is identical to that of an equal number of free molecules.

The anharmonic vibrational Hamiltonian can be modeled by the operator

$$\mathcal{H} = \mathcal{H}^0 + \mathcal{H}'$$

with

$$\mathcal{H}^0 |n\rangle = (n + 1/2)|n\rangle \quad \text{and} \quad \mathcal{H}' = \eta Q^3,$$

using a one-dimensional harmonic oscillator basis $|n\rangle$. In order to calculate intensities of overtones using the above model, a sufficiently large basis must be employed to obtain accurate lower eigenvalues and eigenvectors. n is then varied to yield apparent experimental anharmonicities $\Delta[= (E_{0\to 2} - 2E_{0\to 1})/h\nu]$. In the calculation $0 \leq \Delta \leq 2 \times 10^{-2}$. Assuming only the linear term in eq. 4 is important, it is found that

$$I_{0\to 2}/I_{0\to 1} \approx -0.114\,\Delta \quad .$$

Since in the Born-Oppenheimer approximation the eigenfunctions are still orthogonal, no contributions arise due to the zero order term in equation 4.

A comparison of anharmonicities and intensities in Table 1 indicates that second order transition operators must account for at least 50% of the intensity in any given crystal; one-site operators are expected to be more important than two-site operators. A vapor phase comparison would be enlightening.

The possibility of two successive first order Raman scattering steps yielding photons at $\nu_0 - 2\nu_1$ (ν_0 = laser frequency) is not likely for the following reasons: a) there are significant anharmonicities at least in MoF_6 and WF_6; b) the Raman effect scattering efficiencies are quite small ($\sim 10^{-7}$)[11]; and c) power densities in the focus region yield electric fields of $\sim 10^4$ V/cm which are not large enough to cause significant molecular perturbations for the Raman process.

Since the ν_1 band has a very small (<2 cm^{-1}) dispersion, two-particle states formed in combination with ν_1 will evidence a density of states essentially that of the second vibrational fundamental band. This fact will be exploited in the following sections.

B. ν_2

Figure 1 presents the $\nu_1 + \nu_2$ bands of UF_6 and MoF_6 neat crystals. The lack of any sharp structure indicates two-particle character. While the transitions to the various $\underline{k} = 0$ levels are regulated by separate matrix elements, it is striking that the perturbed band structure from the mixed crystal experiments (shown also in Figure 1) show similar shapes. Neither technique, of course, rigorously displays the correct density of states for ν_2. In neat crystals $\underline{k}$ dependence of transition probabilities across the band cause difficulties while in mixed crystal band states are perturbed by high concentrationsof guest molecules. Nevertheless, both are in substantial agreement. Figure 2 is the calculated density of states of the ν_2 band based on an electrostatic quadrupole-quadrupole interaction. The magnitude of the induced quadrupoles is an adjustable parameter (see paper III, following[4]). The agreement is again favorable. It appears that variation of the scattering intensity to individual two-particle states is small throughout the $\underline{k} = 0$ structure. If single-particle mixing is the important intensity mechanism, then the mixing coefficients must be evenly distributed over the band.

Figure 3 shows the 2 ν_2 overtone band. Again there is no sharp structure and the general shape is similar to the ν_2 density of states just discussed.

If one treats a single branch vibrational exciton band in the limit of small interaction between the separate excitations, the energy of the zero total wavevector or two-particle states is the sum of two (equal energy) fundamental excitons with opposite wavevectors. That is,

$$E_2(\underline{k} = 0, \underline{K} = k') = 2\, E_1(\underline{k}'), \tag{8}$$

and consequently

$$\rho_2(E,0) = \tfrac{1}{2}\rho_1(E/2), \tag{9}$$

in which $E_1(\underline{k}')$, $\rho_1(E)$ and $E_2(\underline{k},\underline{K})$, $\rho_2(E,\underline{k})$ are the fundamental and overtone band energies and densities of states, $\underline{k}$ and $\underline{K}$ are the total and relative wavevectors as described in Sect. IIB., and $\rho_2(E,\underline{k})$ is a partial density of states integrated over $\underline{K}$ but preserving $\underline{k}$. Equation 8 is a consequence of time reversal invariance, $E_1(-\underline{k}) = E_1(\underline{k})$ and the factor of 1/2 in equation 9 is necessary to preserve normalization. An obvious prediction is that the overtone band will be exactly twice the width of the fundamental band and the structure will be identical but on an extended scale as is observed in the 2 ν_1 Raman band. However, the ν_2 band has eight branches. Figure 4 is the total convolution of the calculated ν_2 band under the requirement that the sum of wavevectors equal zero. There is only qualitative agreement in shape with the observed 2 ν_2 band (Fig. 3). Apparently there are branch selection rules which are not understood at this time.

C. ν_3

The $\nu_1 + \nu_3$ or $2\ \nu_3$ Raman bands have not been observed with sufficient intensity to allow a study of their shapes. However, the infrared absorption $\nu_1 + \nu_3$ band of crystalline UF_6 has appeared in the literature[12] and is reproduced in Figure 5. Figure 6 shows the Raman spectra in the ν_3 region of a series of mixed crystals. The two-humped distribution in the infrared spectrum was assigned as site splitting, but can be seen here to be a mapping of ν_3 density of states (times transition operators) since the band has the characteristics of two-particle states.

D. ν_5

Figure 7 presents the $\nu_1 + \nu_5$ bands of UF_6 and MoF_6 neat crystals. Figure 8 shows the electrostatic quadrupole-quadrupole calculation of the density of states. The conclusions reached for the ν_2 band are also valid for ν_5. The mixed crystal spectra are complicated. To support (not prove) the general validity of the observed $\nu_1 + \nu_5$ two-particle shape as a good approximation of the ν_5 density of states some UF_6 in WF_6 mixed crystal spectra are shown in Figure 9. The spectra were observed to change significantly with concentration. A concentration somewhere between the two depicted might give the two-particle shape. The WF_6 in MoF_6 mixed crystal series is not useful for this discussion because an amalgamated ν_5 band is formed as discussed in the following paper.[4]

The 2 ν_5 overtone band was also observed and is presented in Figure 7 of paper I. The computer generated two-particle density of states is presented in Figure 10. There is general agreement in overall shapes, but this is a crude comparison since the features are not well defined. The 36 cm^{-1} FWHH of the UF_6 2 ν_5 band can only be obtained if the ν_5 density of states includes both features observed in the $\nu_1 + \nu_5$ band (Fig. 7). This indicates that the component located at ν_1 + 204.9 cm^{-1} (the low energy component) is not a single particle peak (compare Figures 7, 8, 9, and 10). A puzzling feature of the UF_6 2 ν_5 distribution is the significant upward shift from the predicted location, [observed: $I(2\nu_5)_{max}$ ~450 cm^{-1}; predicted: $I(2\nu_5)_{max}$ ~430 cm^{-1} using $I(\nu_5)_{max}$ ~215 cm^{-1})]. This displacement may, however, be due to interaction of 2 ν_5 with the many two-particle overtone and combination state between 300-450 cm^{-1}.

V. COMPARISON OF MIXED CRYSTAL AND TWO-PARTICLE DENSITY OF STATES TECHNIQUES

Employing mixed crystals for which translational invariance is no longer conserved, it has been possible to observe the breakdown of $\underline{k} = 0$ selection rules. In principle this affords one optical access to the entire Brillioun zone of wavevector space. However, what is actually observed experimentally is that the $\underline{k} = 0$ structure begins to broaden, intensity builds up between the $\underline{k} = 0$ peaks, and new structure develops as the concentration of dopant is increased. A practical and not readily soluble problem is to determine where in this continuum of changing Raman spectra the neat crystal density of states is being displayed faithfully (if at all). If the dopant concentration has become very large, the density of states cannot be that of the neat crystal and if it is too small, the translational symmetry is not completely destroyed. For the vibrations considered, one can see that concentrations of roughly 20 to 30 percent dopant in these crystals give the shapes which agree best with the two-particle band shapes.

Aside from the fact that the correct density of states can be obtained from $(\nu_i + \nu_1)$ combination spectra when they can be observed, there is a real experimental advantage to this method. Only one crystal need be used and no special concentrations need be determined and/or verified. This takes on a more significant meaning when sample preparation becomes a major part of the experimental effort. Limitations are that combination bands must be observable and must have two-particle character. The observation of Raman scattering from overtone and combination bands is experimentally inherently difficult. These transitions are frequently intense in infrared absorption, however.

VI. SUMMARY AND CONCLUSIONS

The major conclusions of this phase of our study are:

1) The major Raman intensity mechanism for the transitions to higher vibrational levels in these crystals is the second order transition operator rather than the first order transition operator acting in conjunction with anharmonic mixing of levels (at least for the ν_1 modes).

2) Many of the combination and overtone bands in these crystals display two-particle character.

3) Accurate information concerning the density of states of a fundamental vibrational exciton band can be obtained from the two-particle band corresponding to combination with the ν_1 mode.

4) The two-particle determined density of states has allowed an evaluation of the appropriate mixed crystal concentration region in which $\underline{k}$ selection rules are significantly destroyed but in which band structure is not greatly altered.

5) Reasonable agreement between quadrupole-quadrupole band structure calculations and $(\nu_1 + \nu_2)$ and $(\nu_1 + \nu_5)$ two-particle data indicate that band-to-band scattering intensity variations are small throughout the $\underline{k} = 0$ structure.

References

1. E. R. Bernstein and G. R. Meredith, Chem. Phys. __, (1977), paper I.
2. J. L. Birman, Phys. Rev. 131, 1489 (1963).
3. A. Ron and D. F. Hornig, J. Chem. Phys. 39, 1129 (1963); J. Cahill, K. L. treuil, R. E. Miller and G. E. Leroi, J. Chem. Phys. 47, 3678 (1967); V. A. Schettino, Chem. Phys. Lett. 18, 535 (1973); D. A. Dows and V. Schettino, J. Chem. Phys. 58, 5009 (1973).
4. E. R. Bernstein and G. R. Meredith, Chem. Phys. __, (1977), paper III.
5. D. A. Dows, in "Physics and Chemistry of the Organic Solid State," Edited by D. Fox, M. M. Labes and A. Weissberger (Interscience, New York, 1963).
6. D. P. Chock and S. A. Rice, J. Chem. Phys. 49, 4345 (1968).
7. (a) E. I. Rashba, J. Exptl. Theoret. Phys. (USSR) 50, 1064 (1966) [Sov. Phys. JETP 23, 708 (1966)];"Physics of Impurity Centers in Crystals" ed. by G. S. Zavt (Tallinn, USSR, 1972) pg. 417.
   (b) E. F. Sheka, Usp. Fig. Nauk 104, 593 (1971) [Sov. Phys. Usp, 14; 484 (1972))], "Physics of Impurity Centers in Crystals, ed. by G. S. Zavt (Tallinn, USSR, 1972) pg. 431.
8. E. B. Wilson, Jr., J. C. Decius and P. C. Cross, "Molecular Vibrations", (McGraw-Hill, New York, 1955).
9. R. Kopelman, Excited States, Ed. by E. C. Lim (Academic Press, 1975), Vol. II, page 34ff.
10. G. R. Meredith, Thesis, Princeton University, 1977.
11. R. Loudon, Adv. Phys. 13, 423 (1964).
12. R. Bougon and P. Rigny, C. R. Acad. Sci. Paris C263, 1321 (1966).

Table 1. Data Pertaining to the ν_1 Fundamental and Overtone Spectra of Neat Crystals Near 77K.

Crystal	Observed ν_1 (cm^{-1})	FWHH (cm^{-1})	Observed $2\nu_1$ (cm^{-1})	FWHH (cm^{-1})	Λ	$I_{o\to 2}/I_{o\to 1}$ [a]
UF_6	663.96	.5	1327.96	1.6	+.00008	.0016
WF_6	772.25	<.3	1542.49	<1.8	-.0026	.0015
MoF_6	742.19	<.3	1482.79	1.2	-.0021	.0008

a. Accuracy probably not better than $\pm$ 50%.

Figure 1. Raman spectra of regions involving ν_2 exciton structure of several crystals at 77K. The two-phonon $\nu_1 + \nu_2$ spectra of neat UF_6 and MoF_6 are shown at bottom. Above are the ν_2 regions of crystals into which WF_6 has been doped to destroy $\underline{k} = 0$ selection rules and display approximate densities of states. The MoF_6 two-phonon spectra were obtained with a signal averager. The 80% concentration is an estimation based on ratios of ν_1 peaks. Note the difference in energy scale dispersions between UF_6 and MoF_6.

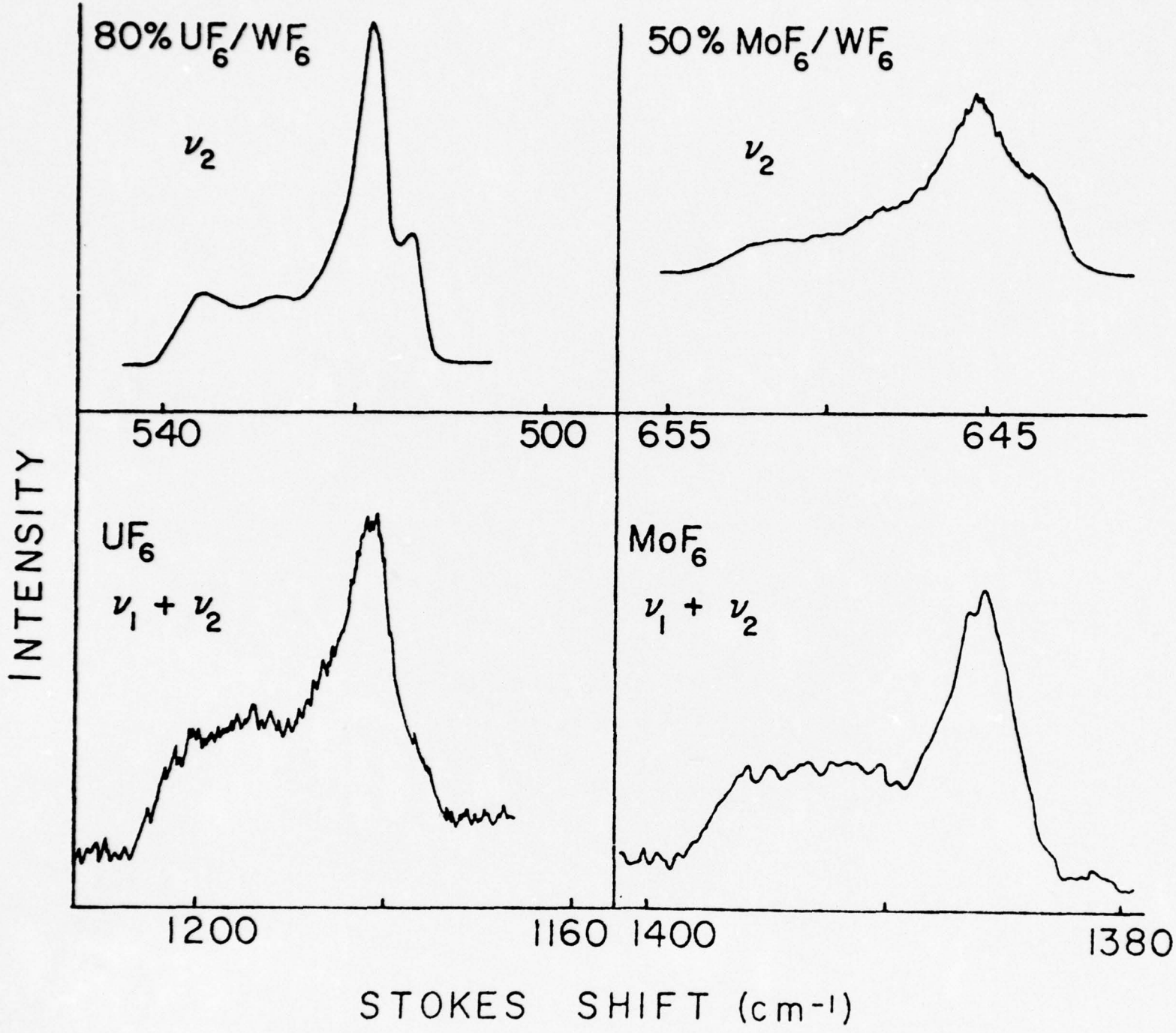
80% UF6/WF6
ν2
540
500
50% MoF6/WF6
ν2
655
645
UF6
ν1 + ν2
1200
1160
MoF6
ν1 + ν2
1400
1380
INTENSITY
STOKES SHIFT (cm-1)

Figure 2. Calculated density of states for the ν_2 exciton band. A quadrupole-quadrupole calculation using the published UF_6 crystal parameters (ref. 4) was performed. The energy scale is directly related to the square of the induced quadrupole moment per unit normal coordinate displacement. The site splitting used in the calculation corresponds to the observed splittings (ref. 4) with the E_g Θ component lower in energy (D_{4h} site model prediction).

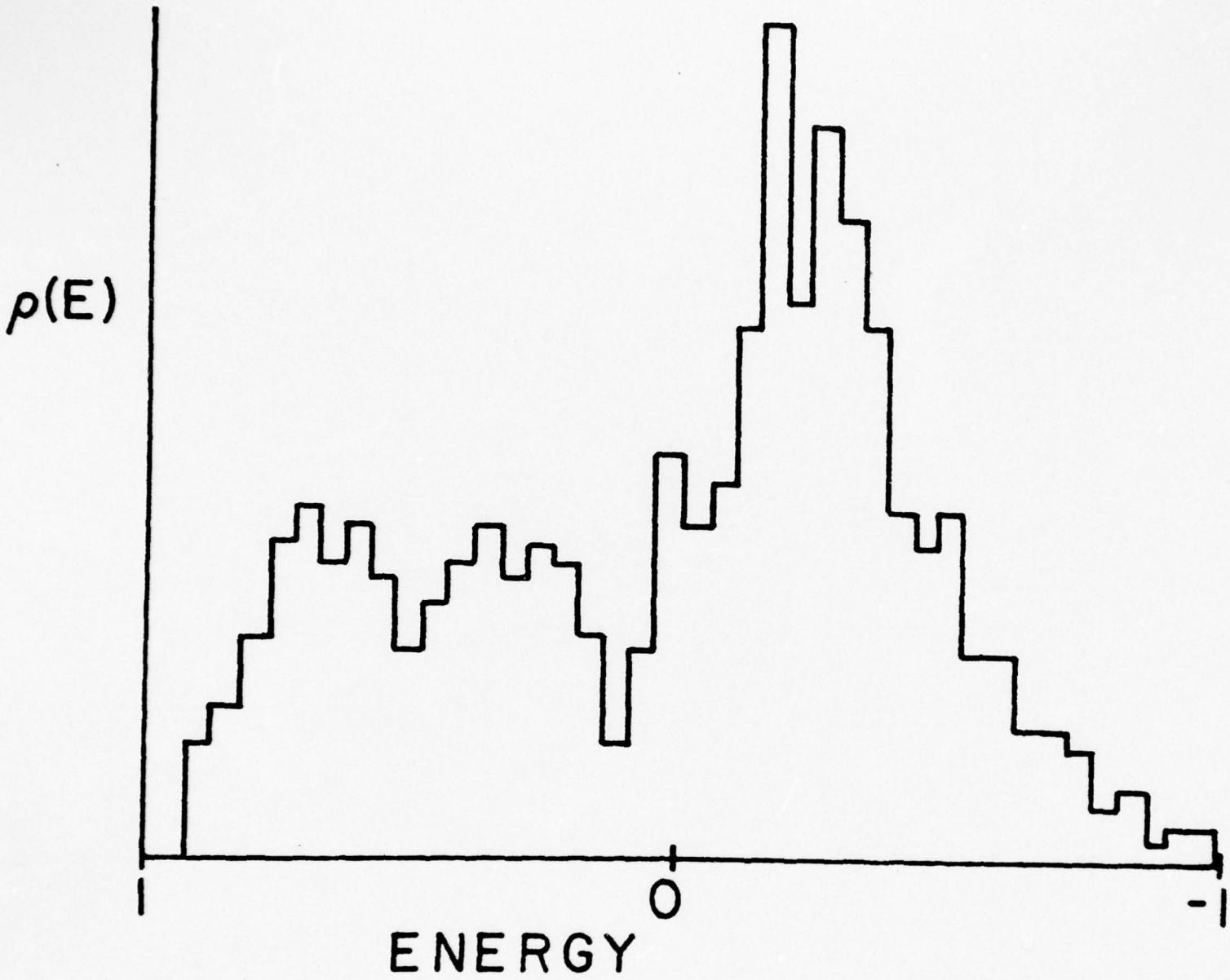
ρ(E)
1
0
-1
ENERGY

Figure 3. Raman spectra of $2\nu_2$ exciton region of neat crystals near 77K. A is UF_6 and B is MoF_6. Note the difference in energy scale dispersions. The MoF_6 spectrum was obtained with a signal averager.

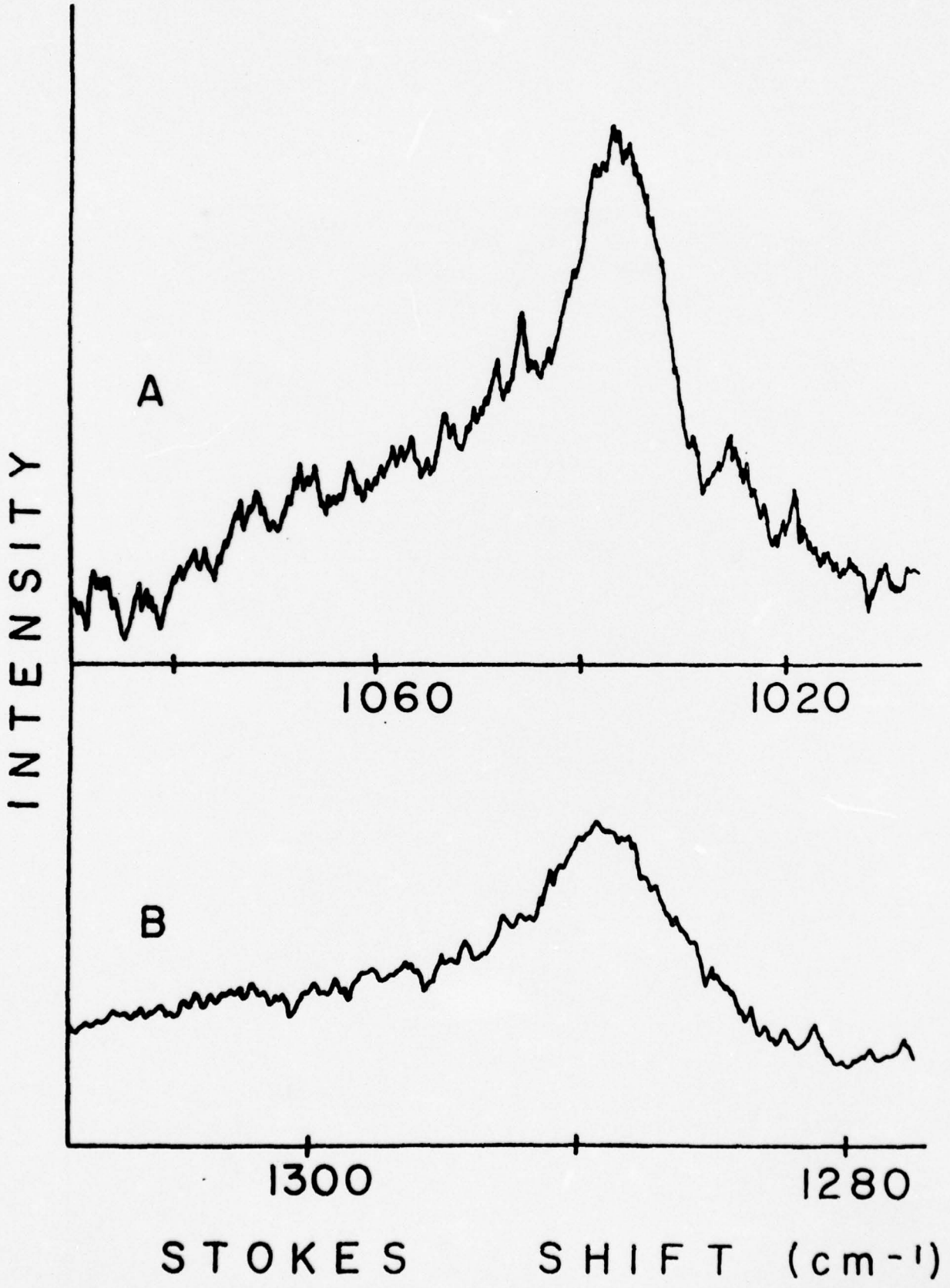
INTENSITY
A
1060
1020
B
1300
1280
STOKES SHIFT (cm-1)

Figure 4. Calculated partial density of states of the $2\nu_2$ two-phonon exciton band. The $\underline{k}$ = 0 two-phonon density of states was constructed from the calculated ν_2 band presented in Figure 2. The energies of the eight branches were summed in pairs under the constraint that the wavevectors sum to zero (or dealing in only one unique octant of this Brillouin zone, requiring that the wavevectors be equal). The $\underline{g}$- and $\underline{u}$-densities are essentially identical except at the zone center and boundaries. $\underline{g}$ or $\underline{u}$ states are those which are symmetric or anti-symmetric when the two-phonon branch labels or wavevectors are interchanged.

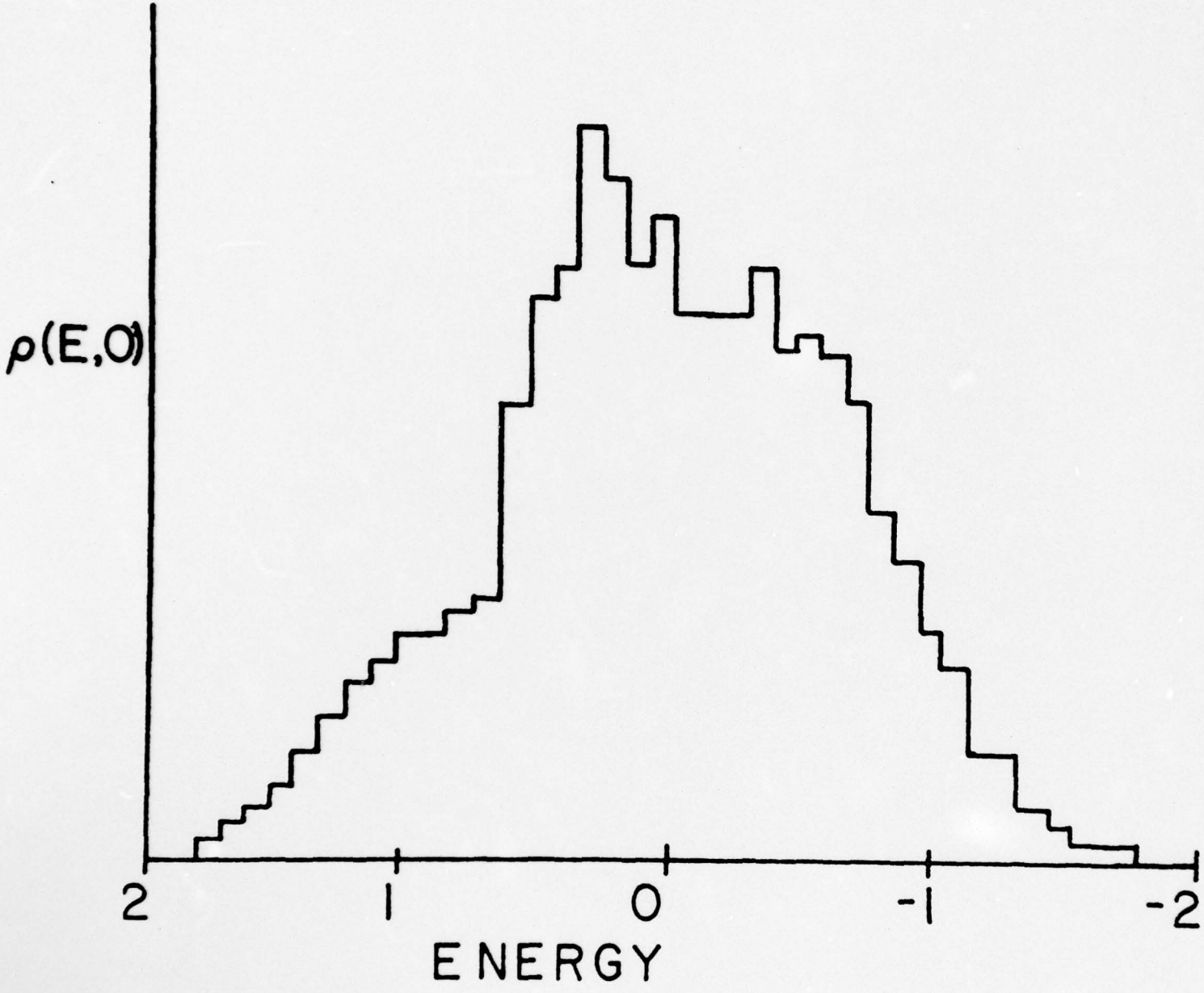
ρ(E,0)
2
1
0
-1
-2
ENERGY

Figure 5. The infrared absorption spectrum of solid UF_6. The spectrum is reproduced from reference 12. It displays the $\nu_1 + \nu_3$ and $\nu_2 + \nu_3$ two-phonon $\underline{k} = 0$ structures.

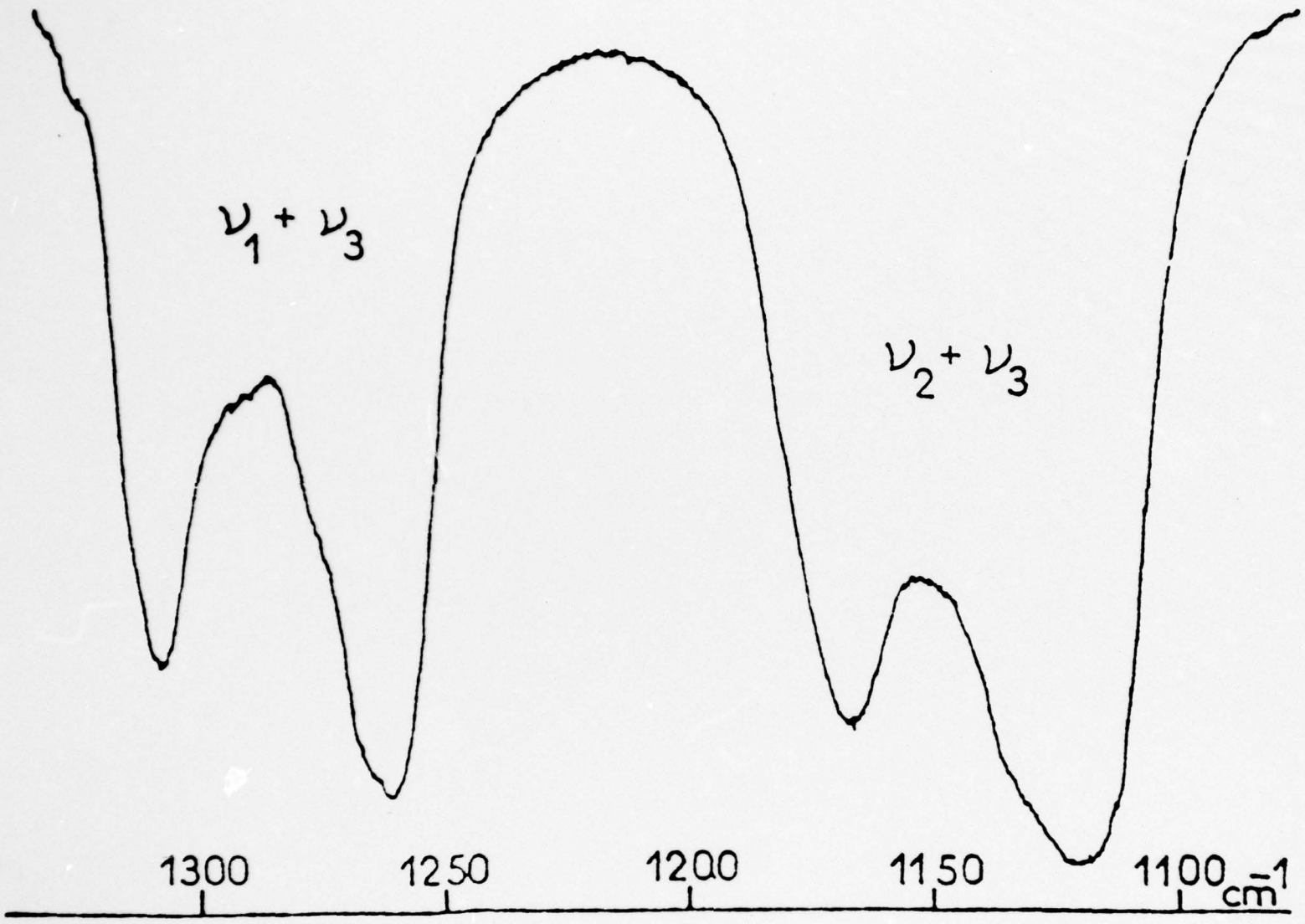
$\nu_1 + \nu_3$
$\nu_2 + \nu_3$
1300
1250
1200
1150
1100
cm⁻¹

Figure 6. Raman spectra of the ν_3 region of UF_6 in various mixed crystals near 77K. The nominal concentration of these crystals were tested by comparison of ν_1 intensities of the two components. The higher energy component in the neat crystal spectrum was discovered only after the mixed crystal spectra and infrared absorption spectra (ref. 12 and Figure 5) were examined.

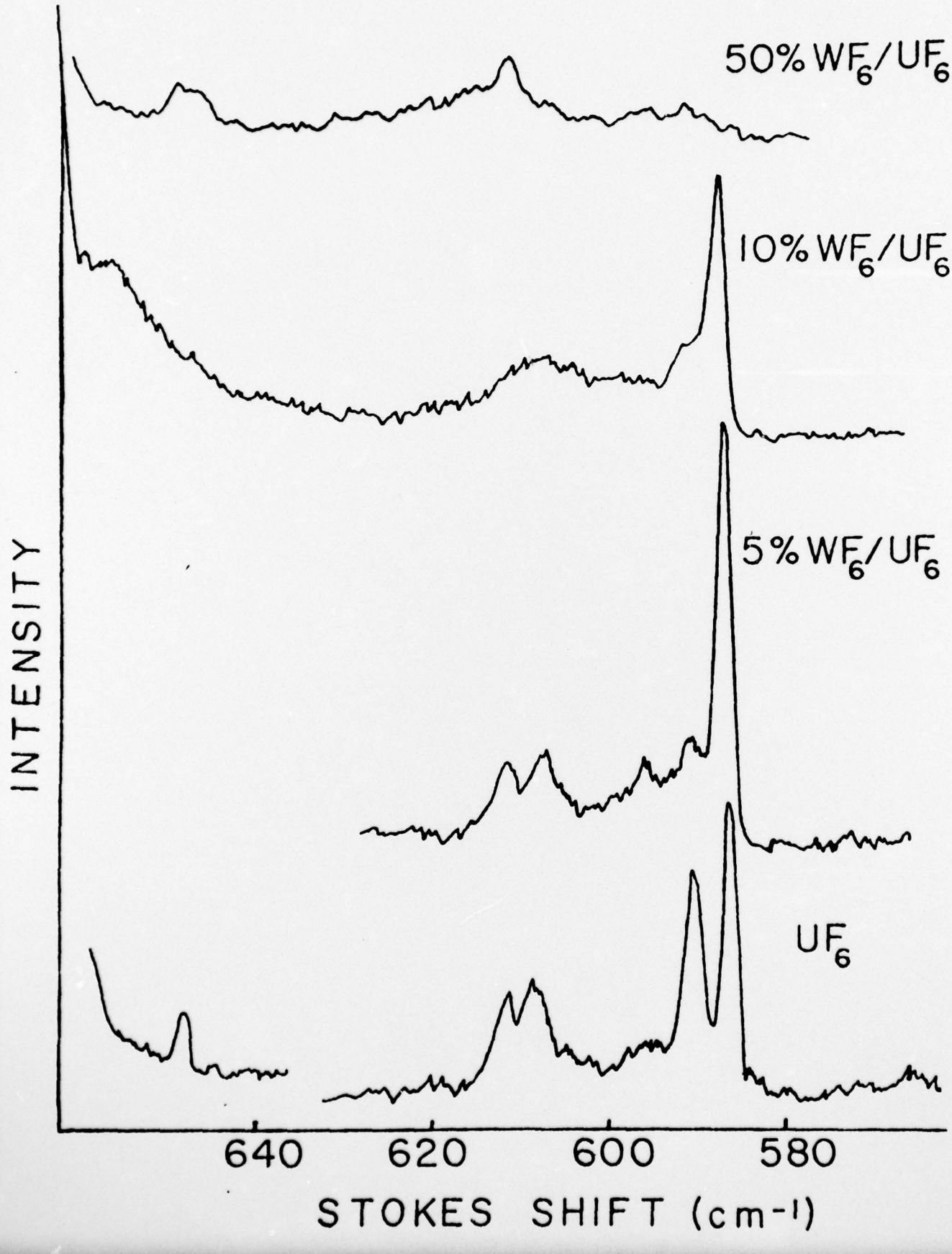
50% WF6/UF6
10% WF6/UF6
5% WF6/UF6
UF6
INTENSITY
640
620
600
580
STOKES SHIFT (cm-1)

Figure 7. Raman spectra of the $\nu_1 + \nu_5$ exciton region of neat crystals near 77K. A is UF_6 and B is MoF_6. The spectra were obtained with a signal averager. Note the difference in energy scale dispersions. The scales are not normalized but nonetheless evidence general similarity of structure.

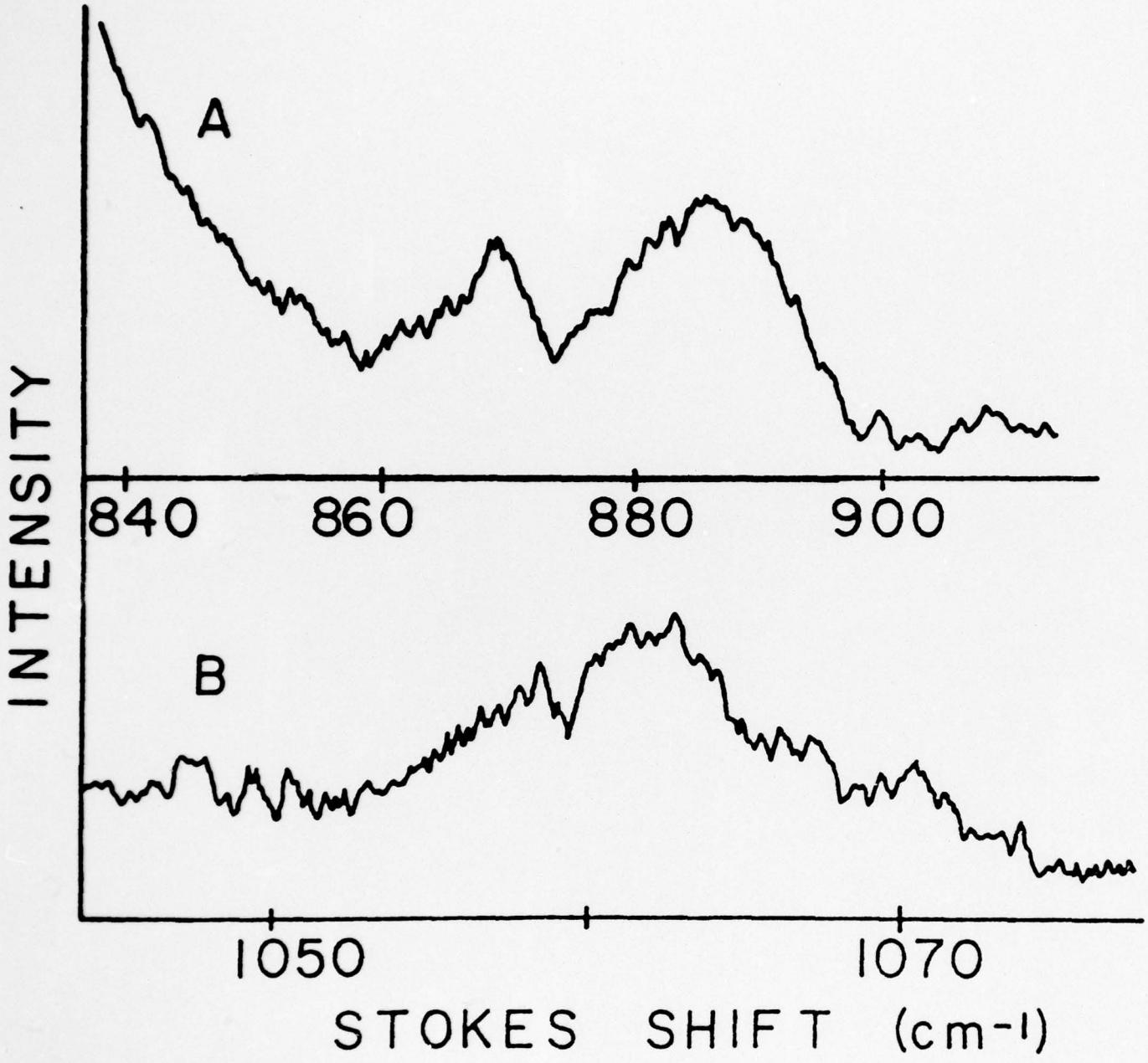
A
B
INTENSITY
840
860
880
900
1050
1070
STOKES SHIFT (cm-1)

Figure 8. Calculated density of states for the ν_5 exciton band. A quadrupole-quadrupole calculation using the published UF_6 crystal parameters (see paper III [4]) was performed. The energy scale is directly proportional to the square of the induced quadrupole moment per unit normal coordinate displacement. The site splitting for this band is in general complex, as discussed in reference 4. In keeping with the D_{4h} site model the component which is b_{2g} in D_{4h} was raised in energy by an amount corresponding to observed splittings in the resolved ReF_6 2μ absorption spectra as reported previously. [E. R. Bernstein and G. R. Meredith, J. Chem. Phys. 64, 375 (1976)].

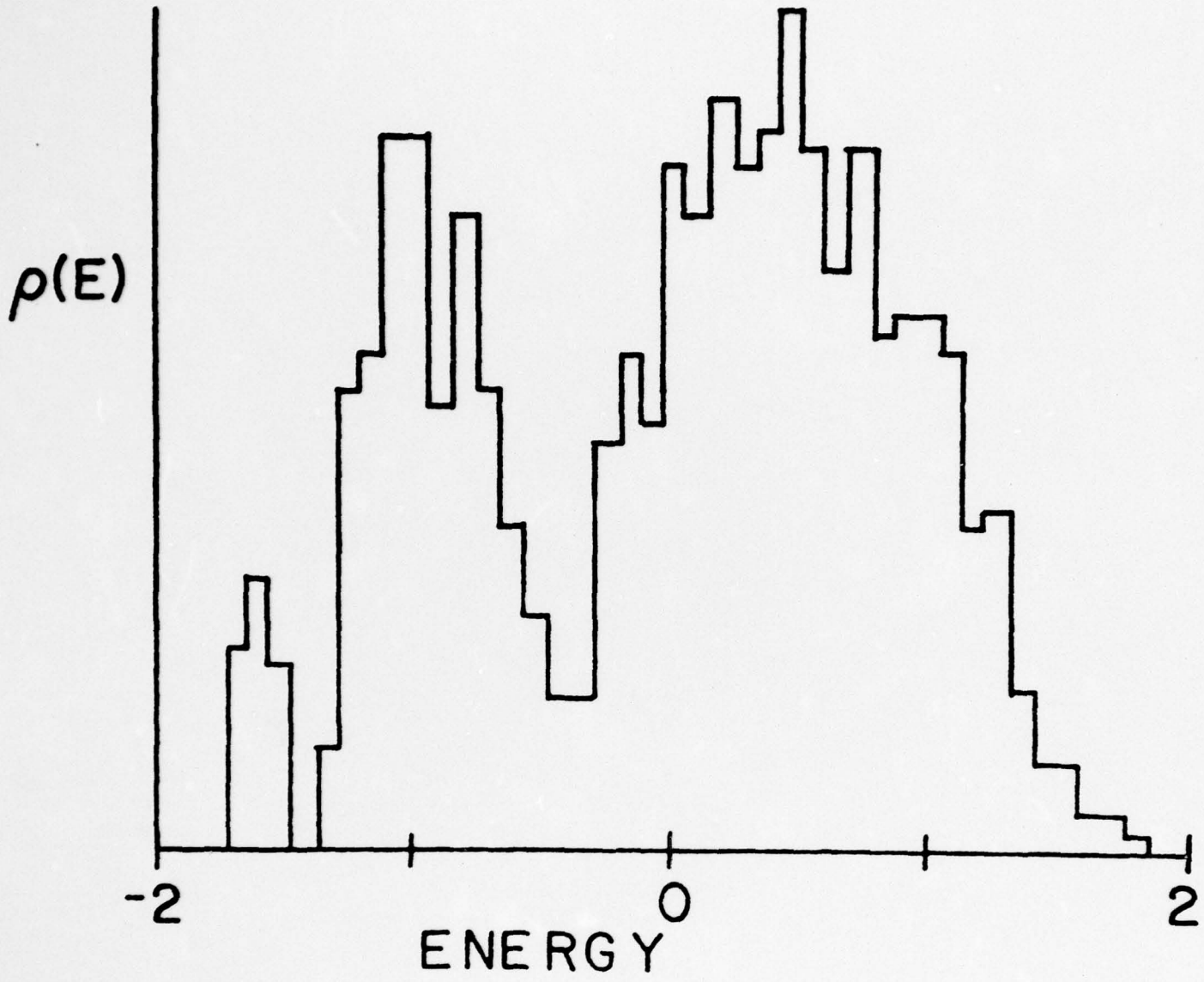
ρ(E)
-2
0
2
ENERGY

Figure 9. Raman spectra of the ν_5 region of UF_6 in mixed crystals near 77K. A is nominally 50% WF_6 in UF_6 while B is nominally 20% WF_6 in UF_6 based on relative ν_1 intensity measurements. Note that the direction of the energy scale is opposite that of Figures 7 and 8. The important point is that intensity shifts from the 220 cm^{-1} region to the 204 cm^{-1} peak as dopant is added. At some intermediate concentration the structure of Figures 7 and 8 may occur.

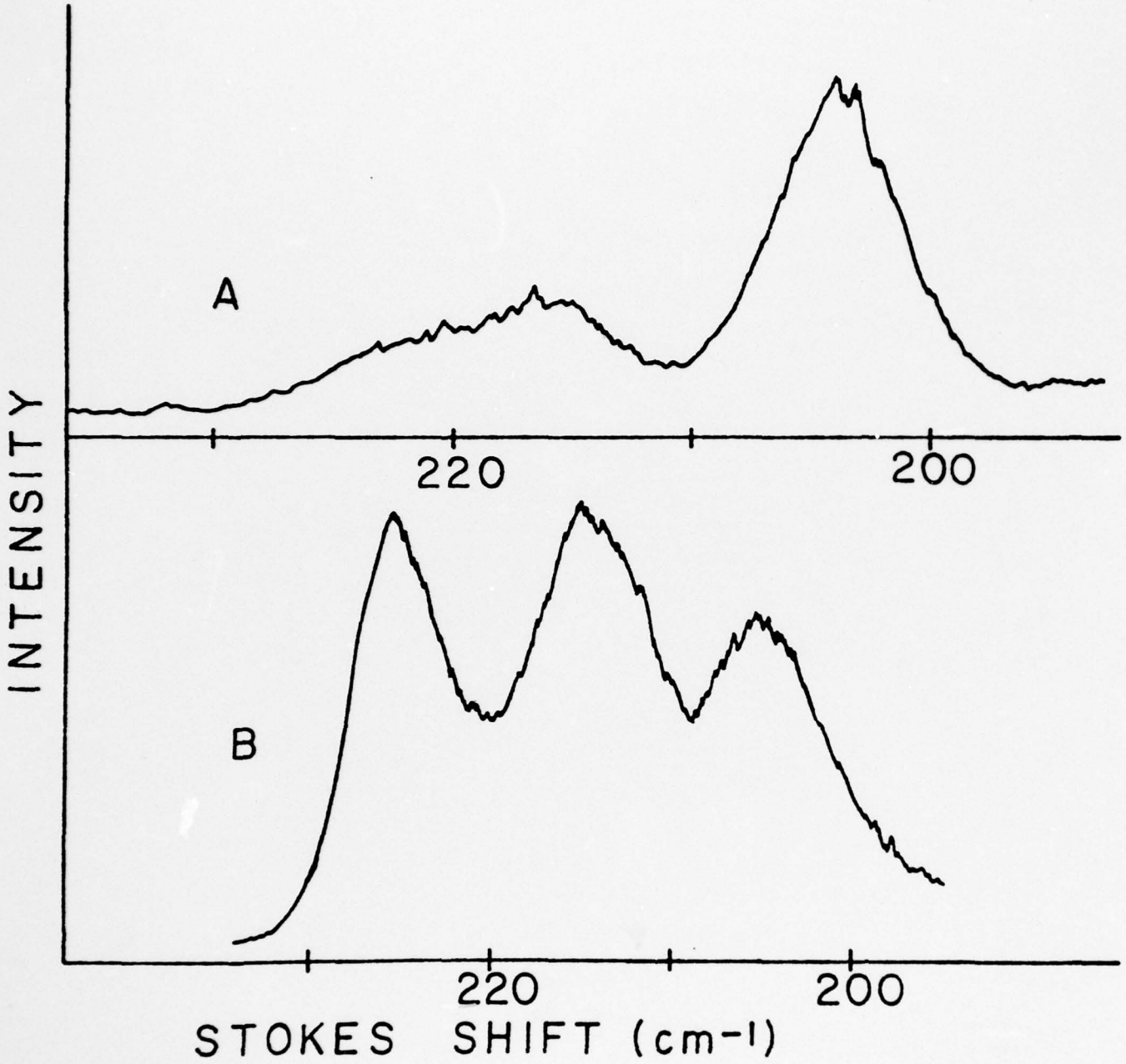
A
220
200
INTENSITY
B
220
200
STOKES SHIFT (cm-1)

Figure 10. Calculated partial density of states of the two-phonon $2\nu_5$ exciton band. The $\underline{k} = 0$ partial density of states for the 12 branch band of Figure 8 was calculated as described in the caption to Figure 4.

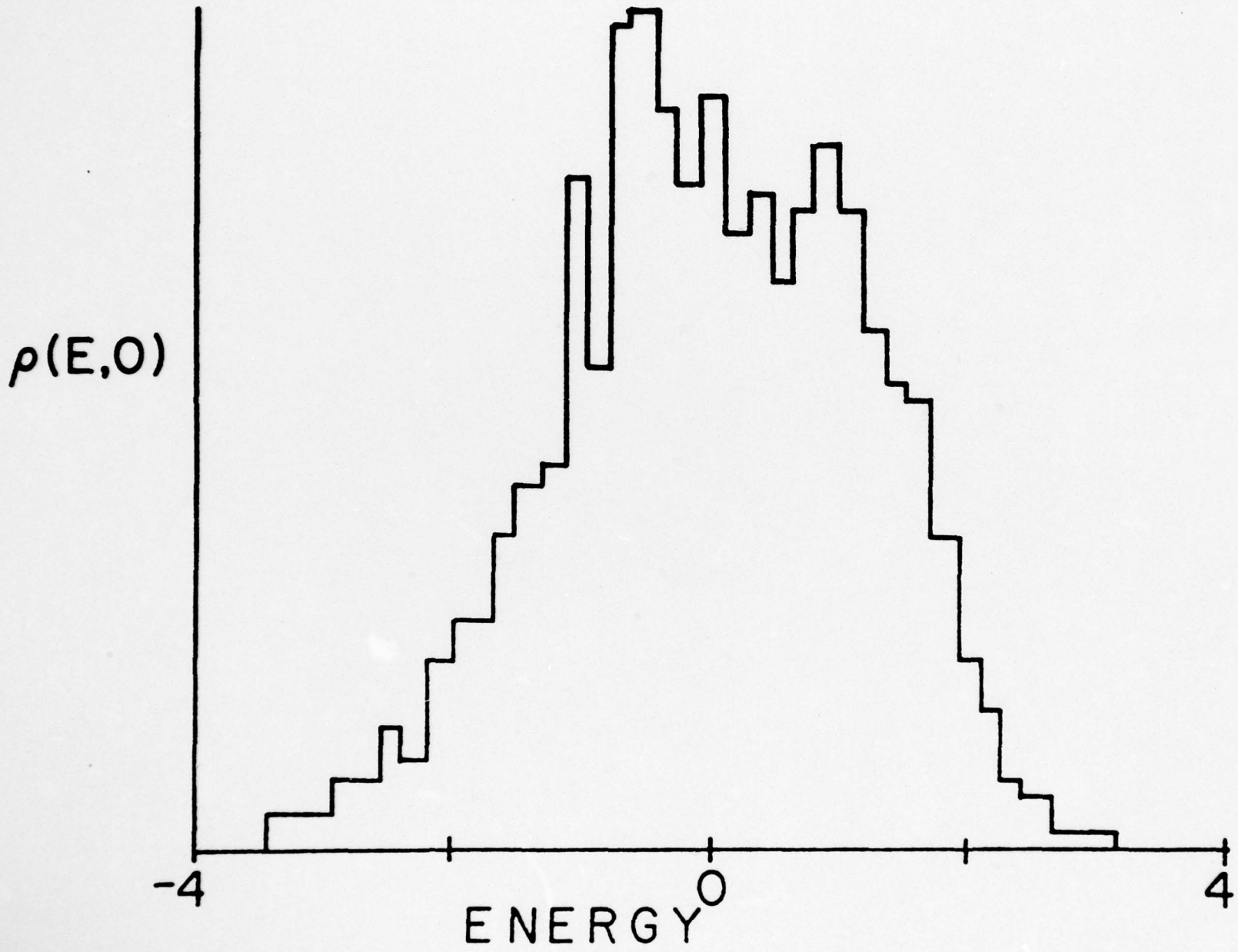
ρ(E,0)
-4
0
4
ENERGY

TECHNICAL REPORT DISTRIBUTION LIST

	No. Copies
Office of Naval Research Arlington, Virginia 22217 Attn: Code 472	2
Office of Naval Research Arlington, Virginia 22217 Attn: Code 102IP	6
ONR Branch Office 536 S. Clark Street Chicago, Illinois 60605 Attn: Dr. George Sandoz	1
ONR Branch Office 715 Broadway New York, New York 10003 Attn: Scientific Dept.	1
ONR Branch Office 1030 East Green Street Pasadena, California 91106 Attn: Dr. R. J. Marcus	1
ONR Branch Office 760 Market Street, Rm. 447 San Francisco, California 94102 Attn: Dr. P. A. Miller	1
ONR Branch Office 495 Summer Street Boston, Massachusetts 02210 Attn: Dr. L. H. Peebles	1
Director, Naval Research Laboratory Washington, D.C. 20390 Attn: Library, Code 2029 (ONRL) Technical Info. Div. Code 6100, 6170	6 1 1
The Asst. Secretary of the Navy (R&D) Department of the Navy Room 4E736, Pentagon Washington, D.C. 20350	1
Commander, Naval Air Systems Command Department of the Navy Washington, D.C. 20360 Attn: Code 310C (H. Rosenwasser)	1

	No. Copie
Defense Documentation Center Building 5, Cameron Station Alexandria, Virginia 22314	12
U.S. Army Research Office P.O. Box 12211 Research Triangle Park, North Carolina 27709 Attn: CRD-AA-IP	
Commander Naval Undersea Research & Development Center San Diego, California 92132 Attn: Technical Library, Code 133	1
Naval Weapons Center China Lake, California 93555 Attn: Head, Chemistry Division	1
Naval Civil Engineering Laboratory Port Hueneme, California 93041 Attn: Mr. W. S. Haynes	1
Professor O. Heinz Department of Physics & Chemistry Naval Postgraduate School Monterey, California 93940	
Dr. A. L. Slafkosky Scientific Advisor Commandant of the Marine Corps (Code RD-1) Washington, D.C. 20380	1

TECHNICAL REPORT DISTRIBUTION LIST

	No. Copies
Dr. M. A. El-Sayed University of California Department of Chemistry Los Angeles, California 90024	1
Dr. M. W. Windsor Washington State University Department of Chemistry Pullman, Washington 99163	
~~Dr. E. R. Bernstein Colorado State University Department of Chemistry Fort Collins, Colorado 80521~~	
Dr. C. A. Heller Naval Weapons Center Code 6059 China Lake, California 93555	1
Dr. G. Jones, II Boston University Department of Chemistry Boston, Massachusetts 02215	
Dr. M. H. Chisholm Chemistry Department Princeton, New Jersey 08540	1
Dr. J. R. MacDonald Code 6110 Chemistry Division Naval Research Laboratory Washington, D.C. 20375	1
Dr. G. B. Schuster Chemistry Department University of Illinois Urbana, Illinois 61801	1
Dr. E. M. Eyring University of Utah Department of Chemistry Salt Lake City, Utah	1
Dr. A. Adamson University of Southern California Department of Chemistry Los Angeles, California 90007	1
Dr. M. S. Wrighton Massachusetts Institute of Technology Department of Chemistry Cambridge, Massachusetts 02139	1